# Probing Surface Noise with Depth-Calibrated Spins in Diamond

B. A. Myers,[1] A. Das,[1] M. C. Dartiailh,[1] K. Ohno,[1] D. D. Awschalom,[1,2] and A. C. Bleszynski Jayich[1]
[1]*Department of Physics, University of California, Santa Barbara, California 93106, USA*
[2]*Institute for Molecular Engineering, University of Chicago, Chicago, Illinois 60637, USA*
(Received 20 February 2014; revised manuscript received 15 May 2014; published 9 July 2014)

Sensitive nanoscale magnetic resonance imaging of target spins using nitrogen-vacancy (NV) centers in diamond requires a quantitative understanding of dominant noise at the surface. We probe this noise by applying dynamical decoupling to shallow NVs at calibrated depths. Results support a model of NV dephasing by a surface bath of electronic spins having a correlation rate of 200 kHz, much faster than that of the bulk N spin bath. Our method of combining nitrogen delta-doping growth and nanoscale depth imaging paves a way for studying spin noise present in diverse material surfaces.

DOI: 10.1103/PhysRevLett.113.027602 PACS numbers: 76.30.Mi, 07.55.Ge, 73.20.-r, 76.60.Jx

The negatively charged nitrogen-vacancy (NV) center in diamond is a robust quantum sensor of magnetic fields [1–4]. Although an individual NV has the capability to detect small numbers of electronic [5–7] and nuclear spins external to diamond [8–10], its widespread application in spin imaging has been limited by the ability to form shallow NVs that retain spin coherence near the surface. Shallow spins with long coherence time $T_2$ are important because quantum phase accumulation between two electronic spin states of the NV provides signal transduction, and hence the minimum detectable magnetic dipole moment scales as $\delta\mu \propto r^3/\sqrt{T_2}$, with $r$ the NV-target spin distance [3,4]. At odds with this figure of merit is strong evidence that the diamond crystal surface adversely affects $T_2$, reducing it from ~2 ms for bulk NVs [11,12] to less than 10 $\mu$s for few-nanometer deep NVs [6,13–16], but the origin of this decoherence is an outstanding question. We consider in this Letter a model of surface spin induced decoherence, a theory that has emerged from experiments on other systems [17,18] where long coherence is a requirement, such as in superconducting circuits [19,20] and spin qubits in silicon [21]. We show that an electronic surface spin model is quantitatively supported for NVs in diamond. The key step we present is to link NV coherence with precise, independently measured NV depth data, as enabled by recent advancements in depth-controlled NV center creation and nanometer-scale magnetic imaging.

Recently, Ohno *et al*. demonstrated shallow, coherent NVs using delta doping of nitrogen during chemical vapor deposition (CVD) of single-crystal diamond (SCD) [16]. This crystal growth technique both permits nanometer-scale depth confinement and minimizes crystal damage incurred during nitrogen ion implantation [13,15,22], the conventional method of generating shallow NVs. The long $T_2$ of these doped NVs has enabled detection of a nanoscale volume of actively manipulated external protons [10]. The consistent NV quality in delta-doped SCD makes depth measurements a suitable probe of surface physics, not masked by effects of other process-induced crystal variations. Therefore, we used this promising material in the reported work: we exploit depth-calibrated NVs to understand how the surface contributes to decoherence and provide a way to mitigate surface noise for enhanced external spin sensing. Using dynamical decoupling (DD) with periodic spacing of $\pi$ pulses for coherence analysis [23], we varied the number of pulses to deduce the noise spectral contributions from the surface and bulk environments as a function of depth. We show that using shorter interpulse spacing can progressively increase efficiency in decoupling from rapid magnetic fluctuations at the surface.

We prepared shallow NVs—all within 160 nm of the surface—in three depth-confined layers of isotopically pure $^{15}$N (> 98%) within an isotopically purified $^{12}$C (99.999%) CVD-grown film, shown schematically in Fig. 1(a). We grew the SCD epitaxially using plasma-enhanced CVD with the conditions and postgrowth NV formation in Ref. [16] and the Supplemental Material [24]. All experiments were performed within a single grown diamond film, thereby eliminating sample-to-sample surface variations. Nanometer scale changes in a NV's depth are critical to both its magnetic sensitivity and spatial resolution; thus, we require an independent method to discriminate NVs' depths beyond the diffraction-limited resolution afforded by standard confocal microscopy [34]. NV-based detection of nuclear spins prepared on the surface can imply an absolute NV depth, though analysis requires an assumed spin magnetic field model and the measurement is time intensive and inaccessible for all but the highest quality NVs sufficiently close to the surface [9,10]. Here we employ a magnetic field gradient assisted optically detected electron spin resonance (ODESR) imaging technique that resolves NV depth differences with nanometer resolution [1,35] over a wide depth range of several hundred nanometers. Moreover, no assumed model is necessary to extract relative NV depths. Absolute depths are inferred by linking this technique with a model of NV coupling to surface spins.

We identify NVs and their depths by combining an inverted confocal microscope and an atomic force microscope

 

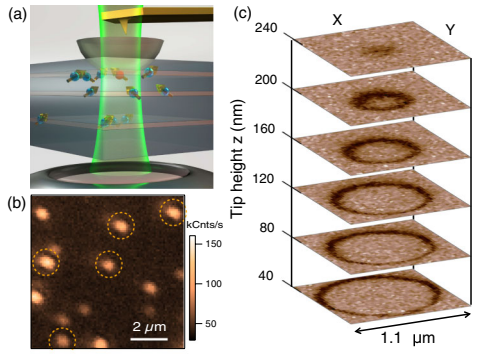


FIG. 1 (color online). (a) Schematic of a CVD-grown diamond film with three nitrogen delta-doped layers (orange) that contain nitrogen-vacancy (NV) spins at nanoscale separations. A 532 nm laser is focused onto NVs via an inverted confocal microscope giving a diffraction-limited depth of field. To achieve nanoscale depth discrimination between NVs, a scanning magnetic tip and microwave field form a resonance slice. Colored red is a NV that intersects this slice. (b) Confocal image showing individual NVs. (c) Optically detected ESR images recorded as a function of the magnetic tip position over a single NV. Dark rings mark reduced fluorescence when the ESR slice crosses the NV.

with a probe magnetized along the tip axis (see the Supplemental Material [24]). Within the film of nitrogen delta-doped layers [Fig. 1(a)] we differentiate doped $^{15}$NVs from bulk, naturally occurring $^{14}$NVs through confocal fluorescence [Fig. 1(b)] and ODESR spectroscopy of the $^{15}$N hyperfine sublevels [16,36]. All data presented in this Letter are on $^{15}$NVs, which are referred to as NVs. To image NV depths, the magnetic AFM tip was scanned over the diamond surface at constant height, producing a bowl-shaped scanning ESR slice near the NVs [Fig. 1(a)]. This slice corresponds to the locus of points in space where the magnetic field along a specified NV axis is constant and brings the NV $|m_s = 0\rangle \leftrightarrow |m_s = -1\rangle$ transition, $\nu_{\mathrm{NV}} = 2.87\ \mathrm{GHz} - \gamma_{\mathrm{NV}}(B_{\mathrm{dc}} + B_{\mathrm{tip}})$, into resonance with a microwave field $\nu_{\mathrm{rf}}$, where $\gamma_{\mathrm{NV}}$ is the NV gyromagnetic ratio and $B_{\mathrm{dc}}$ and $B_{\mathrm{tip}}$ are the externally applied and tip magnetic fields. When a NV intersects the slice, its fluorescence decreases due to its spin-dependent coupling into a long-lived metastable state. In this way, a single NV images the resonant slice, as shown in Figs. 1(c) and 2(a), where the dark contours correspond to the $(x, y, z)$ tip positions for which $\nu_{\mathrm{NV}} \approx \nu_{\mathrm{rf}}$.

We obtained relative depth between any two NVs by registering their $(y, z)$ resonance slice images [Fig. 2(a)] and extracting the vertical offset. The relative depth for a given NV was computed from its mean offset from every other NV, and the standard error of the mean for each NV depth ranged 1–2 nm (see the Supplemental Material [24]). Figure 2(b) is a plot of the Hahn echo coherence envelopes for NVs at four distinct depths, showing $T_2$ decreases with proximity to the surface. The coherence decay envelope of a NV depends on the nature of the environmental spin bath, described by its noise spectral density $\tilde{S}(\omega)$, and the measurement microwave pulse sequence, which applies a filter function to $\tilde{S}(\omega)$. To further isolate the surface-specific contribution we applied higher order DD, specifically $XY4$, to reduce the interpulse spacing $\tau$ for a given total precession time $T$ and thereby decouple the NV from fluctuating fields at frequencies $f < 1/\tau$. Hence, comparing NV coherence subject to different pulse sequences reveals the bath dynamics [37]. The data for $T_{2,\mathrm{echo}}$ and $T_{2,XY4}$ versus depth are plotted in Fig. 2(c) for 13 NVs; the zero depth mark is at an estimated absolute position discussed later. Both $T_{2,\mathrm{echo}}$ and $T_{2,XY4}$ increased nearly monotonically with depth and are suppressed most drastically for depths $< 25$ nm. Importantly, the coherence enhancement $T_{2,XY4}/T_{2,\mathrm{echo}}$ declined from a value of $\sim$2.52 deep in the film to as low as 1.2 for a shallow NV [lower panel of Fig. 2(c)]. This reduced decoupling efficiency of

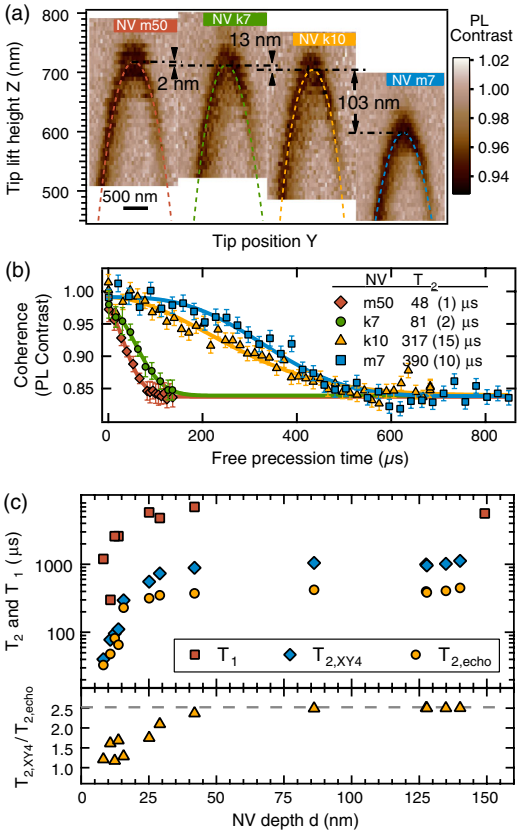


FIG. 2 (color online). (a) ESR slice photoluminescence contrast images in a lateral-height plane ($YZ$) measured for four NVs of identical orientation. Relative depths were extracted via image registration (see the Supplemental Material [24]), and dashed curves are polynomial fits as guides to the eye. (b) Hahn echo coherence data (markers) with shot noise-limited error bars and fits (lines) for the four NVs in (a). (c) Coherence times ($T_{2,\mathrm{echo}}$ and $T_{2,XY4}$) and relaxation times ($T_1$) versus NV depth, showing strong suppression of coherence near the surface. The lower panel shows $T_{2,XY4}/T_{2,\mathrm{echo}} = N^{\lambda}$ is reduced with decreased depth, indicating that dynamical decoupling with $N = 4$ pulses is less efficient for shallower NVs. The dashed line ($\lambda = 2/3$) is expected for NV dephasing by a slow bulk nitrogen spin bath.

NVs near the surface suggests a depth-dependent change in the nature of the dominant spin bath from that of a homogeneous bulk bath to a faster fluctuating configuration of surface spins whose effects are not decoupled at longer precession times. Figure 2(c) also shows that the longitudinal spin relaxation time $T_1$ decreased for shallow NVs over a similar depth scale as the $T_2$ decrease, though $T_1$ was generally an order of magnitude larger than $T_{2,\mathrm{echo}}$. Therefore, $T_1$ processes did not dominate spin decoherence.

To explain the degradation of NV coherence near the surface, we assumed a noise model of pure spin dephasing (see the Supplemental Material [24]). Based on the saturation of $T_2$ in Fig. 2(c) and the isotopically pure $^{12}CH_4$ growth precursor [16], we expected that the dephasing of NVs deep in the film was dominated by interactions with a bulklike spin bath of substitutional nitrogen (P1) centers. Such magnetic noise is well described by a mean field theory with the Ornstein-Uhlenbeck process [23], which phenomenologically has a Lorentzian spectral density centered at zero frequency. It is a natural ansatz to take the total noise spectral density for a NV to be a two-Lorentzian sum with contributions from the bulk and surface

$$\tilde{S}_{\mathrm{bulk}}(\omega)+\tilde{S}_{\mathrm{surf}}(\omega)=\frac{b_{\mathrm{bulk}}^2}{\pi}\frac{\tau_{\mathrm{bulk}}}{1+\omega^2\tau_{\mathrm{bulk}}^2}+\frac{b_{\mathrm{surf}}^2}{\pi}\frac{\tau_{\mathrm{surf}}}{1+\omega^2\tau_{\mathrm{surf}}^2}, \tag{1}$$

where $b_{\mathrm{bulk}}$, $b_{\mathrm{surf}}$ are the NV-noise bath coupling frequencies and $\tau_{\mathrm{bulk}}$, $\tau_{\mathrm{surf}}$ are the baths' autocorrelation times. The dephasing theory predicts a reduced coherence $C_N$ after total NV precession time $T$:

$$C_N(T,b,\tau_c)=\exp\left[-\int_{-\infty}^{\infty}d\omega\tilde{S}(\omega)\mathcal{F}_N(T,\omega)\right], \tag{2}$$

where $\mathcal{F}_N$ is a filter function for the specific $N$-pulse measurement (see the Supplemental Material [24]). We simultaneously fit Hahn echo and $XY4$ coherence decay data to $C_1$ (Hahn) and $C_4$ ($XY4$) and extracted parameters $b_{\mathrm{bulk}}$, $b_{\mathrm{surf}}$, $\tau_{\mathrm{bulk}}$, and $\tau_{\mathrm{surf}}$. For deep NVs ($d>\sim$60 nm) we found that $b_{\mathrm{surf}}$, and thus $\tilde{S}_{\mathrm{surf}}(\omega)$, is negligible, and we determined parameters $b_{\mathrm{bulk}}\approx 13$ kHz and $\tau_{\mathrm{bulk}}\approx 830.2$ $\mu$s (see the Supplemental Material [24]). The $T_{2,XY4}/T_{2,\mathrm{echo}}\approx 2.52$ of these NVs is consistent with $N^{\lambda}$, where $\lambda=2/3$ is expected for a "slow bath" of fluctuating nitrogen spins [23]. This theory predicts from the measured $b_{\mathrm{bulk}}$ a nitrogen density of $\rho_{\mathrm{bulk}}=8.6\times10^{15}$ cm$^{-3}$ (48.5 ppb), also consistent with our mean $T_{2,\mathrm{echo}}=410$ $\mu$s (see the Supplemental Material [24]) and secondary ion mass spectrometry data on nitrogen concentration in the delta-doped films [16].

For spins closer to the surface we fit the coherence envelopes to the full two-bath model of Eq. (2), fixing $b_{\mathrm{bulk}}$ and $\tau_{\mathrm{bulk}}$ to the values found for deep spins. We found a depth-dependent $b_{\mathrm{surf}}$ ranging 3–170 kHz and a depth-independent $\tau_{\mathrm{surf}}=5(3)$ $\mu$s, corresponding to a faster bath than in the bulk and explaining why $T_{2,XY4}/T_{2,\mathrm{echo}}$, and hence $\lambda$, was significantly reduced with NV proximity to the surface. The lack of depth dependence in $\tau_{\mathrm{surf}}$ is consistent with $\tau_{\mathrm{surf}}$ being internal to the bath. The depth dependence of $b_{\mathrm{surf}}$ is well described by a 2D layer of surface $g=2$ spins, and, furthermore, the model yields an absolute NV depth. By integrating over a uniform surface distribution $\sigma_{\mathrm{surf}}$ of fluctuating $S=1/2$ dipoles, we find the total mean square field along the NV axis:

$$B_{\mathrm{rms}}^2=B_{\mathrm{surf}}^2(d)/\gamma_{\mathrm{NV}}^2=\left(\frac{g\mu_0\mu_B}{4\pi}\right)^2\frac{\pi}{4}\frac{\sigma_{\mathrm{surf}}}{(d-d_0)^4}, \tag{3}$$

where $d$ is the relative NV depth (arbitrary zero) and $d_0$ is an offset to find absolute depth (see the Supplemental Material [24]). A fit of Eq. (3) to the $b_{\mathrm{surf}}$ data points in Fig. 3(a) predicts absolute depths $(d-d_0)$ of the shallowest two NVs at 8.2 and 10.8 nm, consistent with the growth rate; the fit error in $d_0$ is $\pm0.5$ nm, and henceforth $d$ denotes absolute depth. We find a surface spin density $\sigma_{\mathrm{surf}}=0.04(2)$ spins/nm$^2$, corresponding to a $r_0\approx 2.8(7)$ nm mean spin separation. The nondiscrete surface spin model is justified because $d\geq r_0$ for all NVs studied here. The depth dependence $b_{\mathrm{surf}}(d)\propto 1/d^2$ is in good agreement with the $b_{\mathrm{surf}}$ data, and by fitting to $b_{\mathrm{surf}}(d)\propto 1/(d-d_0)^{\alpha}$ we find $\alpha=1.8\pm0.2$. We note the importance of measuring a broad depth range of NVs in constraining this exponent (see the Supplemental Material [24]). Figure 3(b) joins the shallow and bulk noise models in a plot of integrated noise power $b^2=b_{\mathrm{bulk}}^2+b_{\mathrm{surf}}^2$, as expressed in magnetic field units as $B^2=b^2/\gamma_{\mathrm{NV}}^2$. The sharp increase in $B^2$ reflects the decrease in spin coherence times at $d<25$ nm in Fig. 2(c), and therefore 25 nm is approximately the depth at which rapidly fluctuating surface spins, rather than the slow P1 spin bath, begin to dominate NV decoherence.

As a cross check of $d_0$ we performed proton sensing on NVs of fitted depths 10.8, 12.4, and 13.8 nm by placing immersion oil on the diamond and using $XY8$-$N$ detection (see Refs. [9,10]). Fitting the proton sensing data corroborates the 10–14 nm depth range of these three NVs (see the Supplemental Material [24]). However, the depth ordering was not consistent with the directly imaged relative depths, raising the question of which NV's depth to fix for $d_0$; hence, we do not use proton sensing measurements to fix $d_0$.

To mitigate surface noise and investigate the validity of our two-bath model we used higher-order DD. We focus here on shallow spins, specifically NV k7 ($d=12.4$ nm), since they are critical for nanoscale magnetometry. For $N\geq 8$, $XY8$-$N$ was chosen for its relevance to those applications. For $N=256$ pulses we measure a $T_2>450$ $\mu$s, corresponding to a magnetic sensitivity of $<10$ nT Hz$^{-1/2}$ (see the Supplemental Material [24]). Figure 4 summarizes the dependence of $T_2$ and decoupling

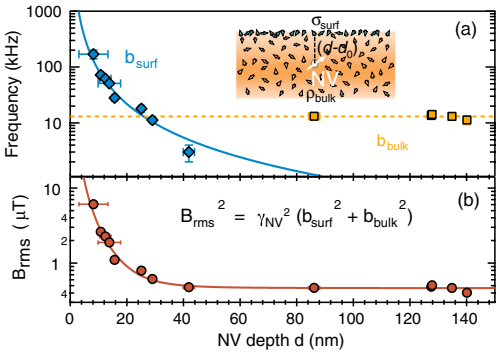


FIG. 3 (color online). (a) Depth dependence of NVs' coupling frequency to the surface (blue diamonds) and bulk (orange squares) noise baths as extracted by fitting coherence decay data to a two-bath dephasing model (see inset schematic). Horizontal error bars on data points denote relative depth errors from the magnetic resonance imaging registration. The solid blue curve is a fit to a 2D electronic spin bath model. The fit gives a surface spin density $\sigma_{\mathrm{surf}} = 0.04\ \mathrm{nm}^{-2}$ and absolute NV depths (shallowest 8.2 nm). (b) Total rms magnetic field of the two spin baths. The solid line is a fit to the two-bath model.

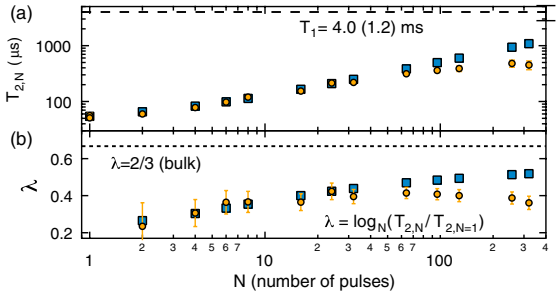


FIG. 4 (color online). The effect of the number of dynamical decoupling pulses $N$ on coherence of a 12.4 nm deep NV. (a) $T_2$ measured using CPMG-$N(N < 8)$ and $XY8$-$N$ (orange circles) and numerical calculations (blue squares) based on the dephasing due to surface and bulk spin baths. The model parameters are $b_{\mathrm{surf}} = 71(4)$ kHz and $\tau_{\mathrm{surf}} = 5(1)\ \mu$s, based on fits to the echo and CPMG-4 data. $T_{2,N}$ error bars ($\delta T_{2,N}$) are coherence fit parameter standard deviations, and the dashed line indicates the measured $T_1$. (b) Plotted is the decoupling efficiency $\lambda$, which relates each $T_{2,N}$ to $T_{2,N=1}$. Error bars are propagated from $\delta T_{2,1}$ and each $\delta T_{2,N}$. The dotted line indicates the measured value of $2/3$ for bulk NVs. The model and data exhibit excellent agreement through $N = 24$.

efficiency $\lambda$ on the number of Carr-Purcell-Meiboom-Gill (CPMG) and $XY8$ pulses up to $N = 320$ [38]. Plotted are the measured data (orange circles) and the calculated, two-bath model prediction (blue squares). There is good quantitative agreement up through $N = 24$, demonstrating that the model captures the low frequency noise spectrum well. The increase in $\lambda$ with $N$ is in contrast with a constant $\lambda_{\mathrm{bulk}} = 2/3$ due to bulk spin noise. As $N$ increases beyond 24, $\lambda$ reaches $\sim$0.42 and then begins to decrease. This behavior is accompanied by a saturating coherence time of $T_{2,N=256} = 480(70)\ \mu$s. The fact that $\lambda$ saturates at a value below $\lambda_{\mathrm{bulk}}$ and does so for an $N$ smaller than the point where $T_{2,N}$ stops increasing could be explained by a second surface related noise source with a correlation time shorter than 5 $\mu$s. This observation is consistent with a recent investigation of diamond surface noise that probed $T_1$ and $T_{1\rho}$ of NVs and reported $\tau_{\mathrm{surf}} = 0.28(3)$ ns assuming a single Lorentzian spectrum [39]. We note, however, that the nonexponential shape and relatively large decoupling efficiency of our coherence data are not explained with this sole GHz correlation rate Lorentzian. We also note that the same study attributed the noise to a surface spin density 0.01 –0.1 spins/nm [39], consistent with our value of $\sigma_{\mathrm{surf}}$, suggesting that both noise sources may arise from the same electronic spin bath.

We have presented a detailed study of decoherence of shallow NVs in a nitrogen delta-doped diamond film. The surface noise is well modeled by a 2D electronic spin layer with sub-MHz dynamics, as evidenced by the depth dependence of coherence enhancement and total noise power probed by NVs at independently measured depths. We have shown that the decohering effects of fluctuating surface and bulk spins in nitrogen delta-doped diamond are mitigated via dynamical decoupling with appropriately chosen interpulse timing, which has significant impact for nano magnetic resonance imaging and coherent spin coupling applications. The extracted $\sigma_{\mathrm{surf}} = 0.04(2)\ \mathrm{spins/nm}^2$ is comparable to the densities found in experiments on metallic and insulating films [18]; the apparent universality of this phenomenon further emphasizes the need to identify the nature of these spins and the mechanism of the bath fluctuations. The scanning magnetic gradient method used here has recently facilitated high-resolution NV-based magnetic resonance imaging of dark spins [40], making NVs an excellent subnanometer spectroscopic probe of this spin noise apparent in a variety of crystal surfaces.

Remaining questions about the diamond surface can be addressed using our method of shallow NV creation via growth combined with nanoscale depth imaging. First, depth-calibrated studies of shallower NVs ($< 5$ nm) may reveal wide variations in $T_2$ from discrete surface spin effects or spin clustering (see the Supplemental Material [24]). Second, using delta doping to form a dark nitrogen spin layer isolated from the diamond surface—$d > 60$ nm based on our findings—could provide a controlled test bed to study 2D spin bath effects on a NV outside the layer. Third, under our present applied magnetic field we expect that NV coupling to electric and strain fields is of second order [41] although experiments at $B_{\parallel} \approx 0$ could probe these effects near the surface. Last, we have presented a two-level dephasing model, but the incompletely understood $T_1$ processes between the $S = 1$ NV sublevels ultimately limit DD as a sensing protocol [42]. $T_1$ measurements of bulk [43] and shallow [39] NVs at lower temperatures suggest thermally activated relaxation rates of surface spins, and a future depth-calibrated study of both $T_1$ and $T_2$ at variable temperature could clarify the mechanism

behind surface spin fluctuations or point to other sources of decoherence. Recently, we learned of current work to probe the diamond surface noise spectrum using the DD method at multiple temperatures [44].

This work was supported by the DARPA QuASAR program and the AFOSR YIP. B. A. M. is supported through a fellowship from the Department of Defense (NDSEG). The authors thank V. V. Dobrovitski, K. Lee, C. McLellan, L. Pascal, D. Rugar, J. Mamin, and S. Kolkowitz for helpful discussions.

[1] G. Balasubramanian, I. Y. Chan, R. Kolesov, M. Al-Hmoud, J. Tisler, C. Shin, C. Kim, A. Wojcik, P. R. Hemmer, A. Krueger, T. Hanke, A. Leitenstorfer, R. Bratschitsch, F. Jelezko, and J. Wrachtrup, Nature (London) **455**, 648 (2008).
[2] C. L. Degen, Appl. Phys. Lett. **92**, 243111 (2008).
[3] J. R. Maze, P. L. Stanwix, J. S. Hodges, S. Hong, J. M. Taylor, P. Cappellaro, L. Jiang, M. V. Gurudev Dutt, E. Togan, A. S. Zibrov, A. Yacoby, R. L. Walsworth, and M. D. Lukin, Nature (London) **455**, 644 (2008).
[4] J. M. Taylor, P. Cappellaro, L. Childress, L. Jiang, D. Budker, P. R. Hemmer, A. Yacoby, R. Walsworth, and M. D. Lukin, Nat. Phys. **4**, 810 (2008).
[5] M. S. Grinolds, S. Hong, P. Maletinsky, L. Luan, M. D. Lukin, R. L. Walsworth, and A. Yacoby, Nat. Phys. **9**, 215 (2013).
[6] B. Grotz, J. Beck, P. Neumann, B. Naydenov, R. Reuter, F. Reinhard, F. Jelezko, J. Wrachtrup, D. Schweinfurth, B. Sarkar, and P. Hemmer, New J. Phys. **13**, 055004 (2011).
[7] H. J. Mamin, M. H. Sherwood, and D. Rugar, Phys. Rev. B **86**, 195422 (2012).
[8] C. A. Meriles, L. Jiang, G. Goldstein, J. S. Hodges, J. Maze, M. D. Lukin, and P. Cappellaro, J. Chem. Phys. **133**, 124105 (2010).
[9] T. Staudacher, F. Shi, S. Pezzagna, J. Meijer, J. Du, C. A. Meriles, F. Reinhard, and J. Wrachtrup, Science **339**, 561 (2013).
[10] H. J. Mamin, M. Kim, M. H. Sherwood, C. T. Rettner, K. Ohno, D. D. Awschalom, and D. Rugar, Science **339**, 557 (2013).
[11] G. Balasubramanian, P. Neumann, D. Twitchen, M. Markham, R. Kolesov, N. Mizuochi, J. Isoya, J. Achard, J. Beck, J. Tissler, V. Jacques, P. R. Hemmer, F. Jelezko, and J. Wrachtrup, Nat. Mater. **8**, 383 (2009).
[12] T. Yamamoto, T. Umeda, K. Watanabe, S. Onoda, M. L. Markham, D. J. Twitchen, B. Naydenov, L. P. McGuinness, T. Teraji, S. Koizumi, F. Dolde, H. Fedder, J. Honert, J. Wrachtrup, T. Ohshima, F. Jelezko, and J. Isoya, Phys. Rev. B **88**,075206 (2013).
[13] B. Naydenov, F. Reinhard, A. Lämmle, V. Richter, R. Kalish, U. F. S. D'Haenens-Johansson, M. Newton, F. Jelezko, and J. Wrachtrup, Appl. Phys. Lett. **97**, 242511 (2010).
[14] P. Maletinsky, S. Hong, M. S. Grinolds, B. Hausmann, M. D. Lukin, R. L. Walsworth, M. Loncar, and A. Yacoby, Nat. Nanotechnol. **7**, 320 (2012).
[15] B. K. Ofori-Okai, S. Pezzagna, K. Chang, M. Loretz, R. Schirhagl, Y. Tao, B. A. Moores, K. Groot-Berning, J. Meijer, and C. L. Degen, Phys. Rev. B **86**, 081406 (2012).
[16] K. Ohno, F. J. Heremans, L. C. Bassett, B. A. Myers, D. M. Toyli, A. C. Bleszynski Jayich, C. J. Palmstrøm, and D. D. Awschalom, Appl. Phys. Lett. **101**, 082413 (2012).
[17] R. de Sousa, Phys. Rev. B **76**, 245306 (2007).
[18] H. Bluhm, J. A. Bert, N. C. Koshnick, M. E. Huber, and K. A. Moler, Phys. Rev. Lett. **103**, 026805 (2009).
[19] R. H. Koch, D. P. DiVincenzo, and J. Clarke, Phys. Rev. Lett. **98**, 267003 (2007).
[20] F. D. Wellstood, C. Urbina, and J. Clarke, Appl. Phys. Lett. **50**, 772 (1987).
[21] T. Schenkel, J. A. Liddle, A. Persaud, A. M. Tyryshkin, S. A. Lyon, R. de Sousa, K. B. Whaley, J. Bokor, J. Shangkuan, and I. Chakarov, Appl. Phys. Lett. **88**, 112101 (2006).
[22] D. M. Toyli, C. D. Weis, G. D. Fuchs, T. Schenkel, and D. D. Awschalom, Nano Lett. **10**, 3168 (2010).
[23] G. de Lange, Z. H. Wang, D. Ristè, V. V. Dobrovitski, and R. Hanson, Science **330**, 60 (2010).
[24] See Supplemental Material at http://link.aps.org/supplemental/10.1103/PhysRevLett.113.027602 for experimental methods and materials, derivation of the equations, and data analysis, which includes Refs [25–33].
[25] L. Childress, M. V. Gurudev Dutt, J. M. Taylor, A. S. Zibrov, F. Jelezko, J. Wrachtrup, P. R. Hemmer, and M. D. Lukin, Science **314**, 281 (2006).
[26] G. de Lange, T. van der Sar, M. Blok, Z. H. Wang, V. V. Dobrovitski, and R. Hanson, Sci. Rep. **2**, 382 (2012).
[27] R. de Sousa, Top. Appl. Phys. **115**, 183 (2009).
[28] M. Guizar-Sicairos, S. T. Thurman, and J. R. Fienup, Opt. Lett. **33**, 156 (2008).
[29] J. H. N. Loubser and J. A. van Wyk, Rep. Prog. Phys. **41**, 1201 (1978).
[30] L. M. Pham, N. Bar-Gill, C. Belthangady, D. Le Sage, P. Cappellaro, M. D. Lukin, A. Yacoby, and R. L. Walsworth, Phys. Rev. B **86**, 045214 (2012).
[31] L. G. Rowan, E. L. Hahn, and W. B. Mims, Phys. Rev. **137**, A61 (1965).
[32] Z. H. Wang and S. Takahashi, arXiv:1209.3365.
[33] M. Loretz, S. Pezzagna, J. Meijer, and C. L. Degen, Appl. Phys. Lett. **104**, 033102 (2014).
[34] A. Gruber, A. Dräbenstedt, C. Tietz, L. Fleury, J. Wrachtrup, and C. von Borczyskowski, Science **276**, 2012 (1997).
[35] M. S. Grinolds, P. Maletinsky, S. Hong, M. D. Lukin, R. L. Walsworth, and A. Yacoby, Nat. Phys. **7**, 687 (2011).
[36] J. R. Rabeau, P. Reichart, G. Tamanyan, D. N. Jamieson, S. Prawer, F. Jelezko, T. Gaebel, I. Popa, M. Domhan, and J. Wrachtrup, Appl. Phys. Lett. **88**, 023113 (2006).
[37] G. de Lange, D. Ristè, V. V. Dobrovitski, and R. Hanson, Phys. Rev. Lett. **106**, 080802 (2011).
[38] We note that cleaning the sample with solvents prior to these measurements resulted in slightly altered coherence times from those presented in Figs. 1–3, which could be attributed to redistribution of surface spins (see the Supplemental Material [24]). Specifically, $T_{2,\mathrm{echo}}(T_{2,XY4})$ changed from 81 (96) to 56(78) $\mu$s for this NV (though other shallow NVs showed increased $T_{2,\mathrm{echo}}$).
[39] T. Rosskopf, A. Dussaux, K. Ohashi, M. Loretz, R. Schirhagl, H. Watanabe, S. Shikata, K. M. Itoh, and C. L. Degen, Phys. Rev. Lett. **112**, 147602 (2014).
[40] M. S. Grinolds, M. Warner, K. De Greve, Y. Dovzhenko, L. Thiel, R. L. Walsworth, S. Hong, P. Maletinsky, and A. Yacoby, arXiv:1401.2674.

[41] F. Dolde, H. Fedder, M. W. Doherty, T. Nobauer, F. Rempp, G. Balasubramanian, T. Wolf, F. Reinhard, L. C. L. Hollenberg, F. Jelezko, and J. Wrachtrup, Nat. Phys. **7**, 459 (2011).

[42] T. H. Taminiau, J. J. T. Wagenaar, T. van der Sar, F. Jelezko, V. V. Dobrovitski, and R. Hanson, Phys. Rev. Lett. **109**, 137602 (2012).

[43] A. Jarmola, V. M. Acosta, K. Jensen, S. Chemerisov, and D. Budker, Phys. Rev. Lett. **108**, 197601 (2012).

[44] Y. Romach, C. Muller, T. Unden, L. J. Rogers, T. Isoda, K. M. Itoh, M. Markham, A. Stacey, J. Meijer, S. Pezzagna, B. Naydenov, L. P. McGuinness, N. Bar-Gill, and F. Jelezko, arXiv:1404.3879v1.